

## Coupling between oxidation state and hydrogen bond conformation in heme proteins

(cytochrome *c*/hemoglobin/myoglobin/cooperativity/histidine)

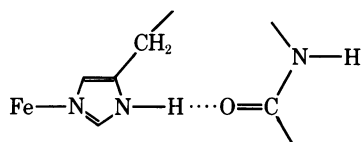
JOAN S. VALENTINE\*, ROBERT P. SHERIDAN†, LELAND C. ALLEN‡, AND PETER C. KAHN§

\*Department of Chemistry, Rutgers, The State University, New Brunswick, New Jersey 08903; †Departments of Chemistry and Biochemical Sciences, Princeton University, Princeton, New Jersey 08540; ‡Department of Chemistry, Princeton University, Princeton, New Jersey 08540; and §Department of Biochemistry and Microbiology, Rutgers, The State University, New Brunswick, New Jersey 08903

Communicated by Walter Kauzmann, December 8, 1978

**ABSTRACT** In all heme proteins for which crystal structures are available, the N<sub>ε</sub> of a histidyl residue is bonded to the heme iron and N<sub>δ</sub> is hydrogen bonded to a carbonyl oxygen of the peptide backbone. We investigate here the possibility that a change in oxidation state of the iron or a change in the geometry of this hydrogen bond might change the hydrogen bond strength in a functionally significant way. Dimerization energies obtained from *ab initio* molecular orbital calculations on the hydrogen-bonded dimer of imidazole and planar formamide are used to represent the strength of this hydrogen bond in heme proteins. The effect of a change in iron oxidation state is modeled by varying the positive charge on imidazole. The effect of a change in hydrogen bond geometry is studied by employing x-ray coordinates for reduced and oxidized cytochrome *c*, deoxy- and metmyoglobin, and deoxy- and methemoglobin. Our conclusions are that the strength of this hydrogen bond in heme proteins is sensitive to both the oxidation state of the iron atom and to geometry changes on the order of those obtained from the x-ray coordinates. We speculate that the changes in oxidation state may be functionally coupled with changes in hydrogen bond geometry and that this hydrogen bond represents a feasible pathway to link protein conformation with redox potential or reactivity of the iron atom.

Imidazole rings of histidyl residues are bound to the metal in a large number of metalloproteins (1). In those proteins for which high resolution x-ray crystal structural data are available, the metal-bound imidazole rings are invariably found to be hydrogen bonded to electronegative groups on the apoprotein (2-4). The possibility that this hydrogen bond might link the tertiary structure of the protein with the reactivity of the metal has been recognized by several investigators, particularly in the case of heme proteins (5-12) in which the electronegative group is a backbone carbonyl oxygen.



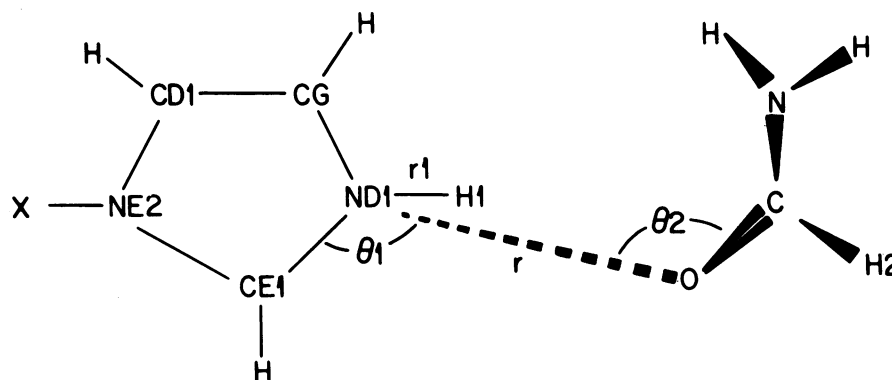
It is well known from studies of model compounds and of imidazole complexes of methemoglobin and metmyoglobin that the pK<sub>a</sub> of imidazole can drop several pH units upon complexation with a metal ion (1) [imidazole pK<sub>a</sub> = 14 (1), metmyoglobin imidazole pK<sub>a</sub> ≈ 10 (13)]. It is also known that in general an increase in the oxidation state of a metal will result in a decrease in the pK<sub>a</sub> of coordinated imidazole (1). It thus seems an inescapable conclusion that a change in oxidation state of iron in a heme protein will affect the nature of this hydrogen bond to some degree. However, the significance of such an

effect cannot be judged without some knowledge of the magnitude of the energies involved. This paper describes an approach to estimating the magnitudes of changes in such hydrogen bond energies in heme proteins, resulting from either (i) changes in the oxidation state of the metal, or (ii) changes in the hydrogen bond geometry due to changes in the tertiary structure of the protein.

Estimates of energies are obtained from *ab initio* molecular orbital calculations of the dimerization energies ( $E_D$ ) of hydrogen-bonded dimers of imidazole and planar formamide (see Fig. 1). Instead of a metal atom, we use an atom X with a hydrogen orbital and a variable nuclear charge. This allows us to investigate the effect of a change in the oxidation state of the iron. The effects of changes in hydrogen bond geometries are investigated by calculations of  $E_D$  for different orientations of imidazole and formamide within the dimer. The dimer geometries that we use are suggested by x-ray crystallographic data for those heme proteins (14-20) for which coordinates are available for two oxidation states<sup>†</sup> (see Table 1). Uncertainties in x-ray coordinates, even in the available highly refined protein x-ray crystal structures, make it impossible to conclude that the observed changes in hydrogen bond geometry actually occur; they could equally well be the result of imprecision in the crystallographic or real-space refinement (21). Nevertheless, the geometries described by the coordinates provide the best available model for the actual protein geometries. The calculations described below indicate that the strength of the hydrogen bond between the metal-bound histidyl imidazole ring and the peptide carbonyl oxygen is markedly sensitive to the charge on the imidazole ring and therefore to the oxidation state of the iron atom. The calculations indicate further that the magnitude of this effect on the hydrogen bond strength is dependent on the hydrogen bond geometry. These results are in fact expected from previous calculations of the charge and geometry dependence of hydrogen-bonded dimers in general (22, 23). We therefore suggest that these two effects may be functionally coupled—i.e., that changes in the oxidation state of the metal will change the strength of this hydrogen bond and that this in turn will lead to changes in hydrogen bond geometry. It necessarily and conversely follows that tertiary structural changes affecting the hydrogen bond geometry will influence the relative stabilities of the oxidation states of the metal. On the basis of these few examples, mechanisms are proposed by which the coupling might contribute to the modulation of redox potentials in cytochromes and of cooperative binding of ligands in hemoglobin. Only after many additional heme proteins have been studied both by our methods and by experiment will it be possible to determine whether the coupling does in fact have general functional significance. At the end of the paper, we

The publication costs of this article were defrayed in part by page charge payment. This article must therefore be hereby marked "advertisement" in accordance with 18 U. S. C. §1734 solely to indicate this fact.

<sup>†</sup> The source for all coordinates used in this study was the Brookhaven Protein Data Bank.



$r$	ND1 - O	DISTANCE
$\theta_1$	CE1 - ND1 - O	ANGLE
$\chi_1$	NE2 - CE1 - ND1 - O	DIHEDRAL ANGLE
$\theta_2$	ND1 - O - C	ANGLE
$\chi_2$	CE1 - ND1 - O - C	DIHEDRAL ANGLE
$\chi_3$	ND1 - O - C - H2	DIHEDRAL ANGLE

FIG. 1. The hydrogen bonded imidazole-formamide dimer used for calculations of the dimerization energies with internal coordinates defined. The nomenclature for the atoms in the imidazole ring is that for histidine used by the Brookhaven Protein Data Bank.

mention other classes of proteins in which hydrogen bonds may play similar roles.

#### Examination of the x-ray structures

In all heme proteins for which crystal structures are available,  $N_\epsilon$  (called NE2 in Fig. 1) of histidine is bonded to iron and  $N_\delta$  (called ND1) is found to be hydrogen bonded to a carbonyl oxygen of the peptide backbone. In order to obtain specific information about the geometry of the hydrogen bond, scale models of the region surrounding the iron-bound histidine have been built for those proteins listed in Table 1. Visual comparison of the reduced (ferrous) form with the oxidized (ferric) form of each protein shows that substantial changes in hydrogen bonding geometry are required by the x-ray coordinates of several of the proteins. In order to describe the hydrogen bond geometry in the model imidazole-formamide dimer used in

our calculations, internal coordinates were defined as shown in Fig. 1. Values for each internal coordinate are derived from the Cartesian coordinates of the corresponding atoms of the protein. The ND1-O-C-CA dihedral angle is taken for  $\chi_3$ , in which CA is the  $\alpha$  carbon adjacent to the carbonyl carbon atom of the peptide group (in the model H2 replaces CA). When the ND1-O-C-CA angle differs from the ND1-O-C-N angle by other than  $180^\circ$  (indicating an apparent nonplanarity in the carbonyl group, which was never found to be more than  $15^\circ$ ), we symmetrically adjust the angles and use the adjusted value for  $\chi_3$ . The internal coordinates obtained in this way are listed in Table 1. Comparison of the internal coordinates of redox pairs of proteins shows that the most pronounced changes occur in cytochrome *c* and in the  $\alpha$  chain of hemoglobin. In cytochrome *c* the hydrogen bond heavy atom distance  $r$  (see Fig. 1) shortens by 1 Å in going from the reduced to the oxidized

Table 1. Internal coordinates\* for the hydrogen-bonded residues of several redox pairs of heme proteins

Protein	Source	Hydrogen-bonded residues	$r$ , Å	$\theta_1$ , °	$\chi_1$ , °	$\theta_2$ , °	$\chi_2$ , °	$\chi_3$ , °
Cytochrome <i>c</i> <sup>†</sup>	Tuna	His-18---Pro-30	3.515	116	175	151	28	17
		Oxidized, outer	2.486	112	191	158	26	9
		Oxidized, inner	2.374	117	170	146	55	351
Myoglobin <sup>‡</sup>	Sperm whale	His-93---Leu-89	2.760	144	202	131	16	323
		Met-	2.791	143	207	135	2	333
Hemoglobin <sup>§</sup>	Horse	His-87---Leu-83	2.634	104	201	139	231	113
		$\alpha$ met-	2.756	135	182	143	22	318
		$\beta$ deoxy-	2.703	148	205	121	19	301
		$\beta$ met-	2.664	137	196	142	23	308

\* The internal coordinates are defined in Fig. 1.

<sup>†</sup> Refs. 14–16. Oxidized cytochrome *c* exists in the crystal as two crystallographically distinct molecules, outer and inner.

<sup>‡</sup> Refs. 17, 18.

<sup>§</sup> Refs. 19, 20.

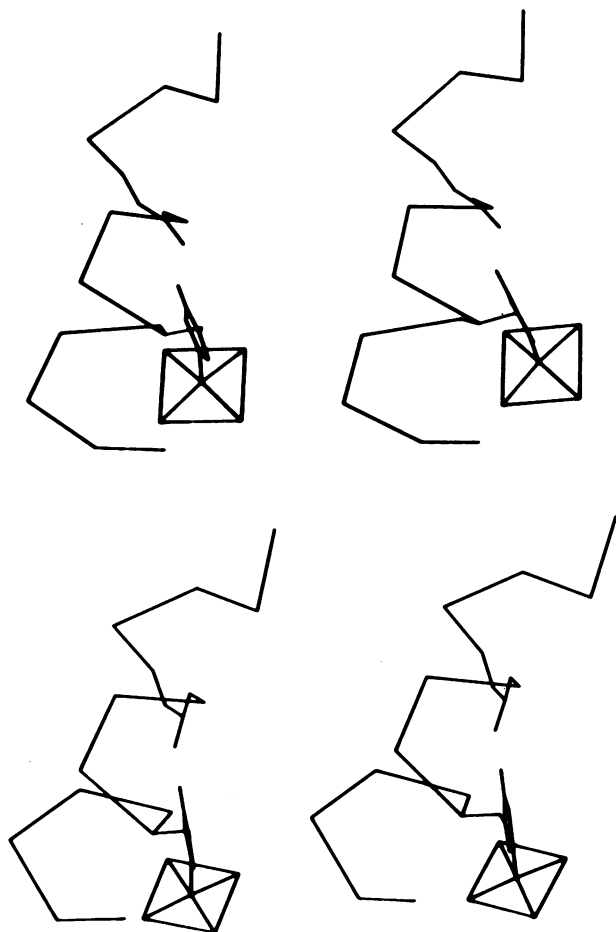


FIG. 2. Stereoscopic images of axial imidazole hydrogen bonds in the  $\alpha$  chains of horse deoxy- and methemoglobin. Section of F helix backbone from Ala-79 through Arg-92. For Leu-83 all nonhydrogen backbone atoms are drawn. For Ser-84 the peptide nitrogen and  $\alpha$  carbon are shown. The carbonyl of Leu-83 is the hydrogen bond acceptor for the axial histidine. For all other residues only  $\alpha$  carbons are drawn. The imidazole hydrogen is located as in the text. The heme is represented by the iron and by a square connecting the four pyrrole nitrogens. (Upper) Deoxy- $\alpha$  chain. The oxygen of the Leu-83 carbonyl is seen to be out of the imidazole ring plane. (Lower) Met- $\alpha$  chain. Note that the carbonyl oxygen is nearly colinear with the N—H bond.

forms. In the hemoglobin  $\alpha$  chain (see Fig. 2)  $\theta_1$  goes from  $104^\circ$  in deoxy- to  $135^\circ$  in met- and  $\chi_1$  goes from  $201^\circ$  in deoxy- to  $182^\circ$  in met- (a linear hydrogen bond would have  $\theta_1 = 128^\circ$  and  $\chi_1 = 180^\circ$ ). We shall use these changes in hydrogen bond geometry suggested by the x-ray coordinates to investigate the effect of such geometrical changes on the strength of the hydrogen bond. We emphasize that, due to the uncertainties in the x-ray data, these changes in hydrogen bond geometry may not be the same as those actually occurring in the proteins.

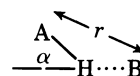
### Calculation of dimerization energy

*Ab initio* calculations of the dimerization energies for hydrogen bonded dimers of imidazole and planar formamide have been carried out. Monomer geometries for imidazole (24) and formamide (25) are taken from small molecule crystallography and kept fixed unless otherwise stated. The atom X is fixed along the CE1-NE2-CD1 angle bisector at a distance of 1.03 Å, the optimized distance for nuclear charge equal to 1.0 on atom X (this distance is not a sensitive parameter in the model). The relative orientations of imidazole and formamide in the

hydrogen-bonded dimer are fixed, using the six internal coordinates derived from the x-ray coordinates; they are listed in Table 1. We optimize by energy minimization only the ND1-H1 distance,  $r_1$ , because it is the principal critical distance that varies with charge on the system; of course this distance is unavailable from crystallography.

The calculations were made by the self-consistent field molecular orbitals as linear combinations of atomic orbitals (SCF-MO-LCAO) method using the STO-3G basis set with the standard digital computer program GAUSSIAN 70 (26), modified for variable nuclear charges. A hydrogen basis orbital was assigned to X. Dimerization energies were calculated by subtracting the energies of the formamide and optimized imidazole monomers from the energy of the dimer. These are listed in Table 2. More positive values of  $E_D$  indicate stronger hydrogen bonds.

The geometry of the imidazole-formamide hydrogen bond is best discussed in terms of the parameters  $r$ , the hydrogen bond heavy atom distance, and  $\alpha$ , the angular deviation from linearity.



Previous high accuracy molecular orbital calculations (22, 23) on hydrogen-bonded dimers of small hydrides have shown that, for a given proton donor A and electron donor B,  $E_D$  is proportional to  $\cos \alpha/r$  when  $r$  is near its equilibrium value,  $r_{eq}$ . More highly charged systems, whether anionic or cationic, characteristically have higher  $E_D$  values and shorter  $r_{eq}$  values than the corresponding neutral systems. In the imidazole-formamide system that we study here,  $E_D$  obeys the  $\cos \alpha/r$  rule for values of  $\alpha$  and  $r$  that were derived from x-ray coordinates.

Table 2. Dimerization energies

Protein	Dimerization energies, kcal/mol		
	Neutral dimer ( $Z_X = 0.0$ )	Cationic dimer ( $Z_X = 1.0$ )	Cationic - neutral
Cytochrome <i>c</i>			
Reduced	3.8	10.9	7.1
Outer	3.2	21.8	18.6
Inner	1.2	25.6	24.4
Outer - reduced	-0.6	10.9	11.5
Inner - reduced	-2.6	14.7	17.3
Myoglobin			
Deoxy-	7.8	21.1	13.3
Met-	7.3	20.0	12.7
Met- - deoxy-	-0.5	-1.1	-0.6
Hemoglobin			
$\alpha$ deoxy-	2.9	15.8	12.9
$\alpha$ met-	9.2	24.8	15.6
$\alpha$ met- - deoxy-	6.3	9.0	2.7
$\beta$ deoxy-	6.4	18.9	12.5
$\beta$ met-	8.5	25.1	16.6
$\beta$ met- - deoxy-	2.1	6.2	4.1

One kcal = 4.184 kJ.

### Effect of change in metal oxidation state

The effect on the hydrogen bond energy of a change in the oxidation state of the iron is modeled by varying the nuclear charge of X ( $Z_X$ ) between 0.0 and 1.0 while keeping the geometry fixed. Because the number of electrons in the system remains constant, the value of  $Z_X = 0$  corresponds to the neutral dimer and the value of  $Z_X = 1$  corresponds to the fully cationic dimer. It is expected that the charge on the atoms involved in the hydrogen bond in our proteins will fall between these limiting cases, the reduced forms being closer to the neutral dimer and the oxidized forms being closer to the cationic dimer. Exactly how much the charge on the hydrogen bond differs between reduced and oxidized heme proteins is uncertain. It is known from experiment that the bonding of imidazole to transition metal complexes does not cause as large a drop in  $pK_a$  as that caused by the bonding of imidazole to a proton (1). Thus, it is likely that the positive charge residing on this hydrogen bond in ferric heme proteins is somewhat less than 1.0. The results of our calculation (see Table 2) indicate that  $E_D$  is 7–17 kcal/mol greater in the cationic dimer than in the neutral dimer. Moreover, calculations with intermediate values of  $Z_X$  indicate that, for any fixed geometry,  $E_D$  increases nearly linearly with  $Z_X$ . The magnitude of the change in  $E_D$  caused by a change in  $Z_X$  is, of course, dependent on the geometry. The more favorable the hydrogen bond geometry, the greater will be the increase in  $E_D$  produced by the change in  $Z_X$  (i.e., cationic minus neutral in Table 2).

### Effect of geometry changes

Calculations of  $E_D$  were carried out for each geometry given by the protein coordinates with  $Z_X$  fixed first at 0.0 and then at 1.0. The results in Table 2 show that the changes in the hydrogen bond on going from the geometry of the reduced form to that of the oxidized form for each redox pair can cause changes in  $E_D$  as great as 14.7 kcal/mol when  $Z_X = 1.0$  and 6.3 kcal/mol when  $Z_X = 0.0$ .

Variation in the strength of the hydrogen bond with geometry as well as with charge is consistent with the general properties of hydrogen bonds discussed above. It is interesting to note that for each redox pair except myoglobin (where the differences in geometry are not significant), the oxidized form of the protein as described by the x-ray coordinates has a more favorable hydrogen bond geometry than the reduced form. This is what we would predict should be observed if the oxidation state of the metal is coupled to the tertiary structure of the protein through the intermediacy of this hydrogen bond, higher charges differentially stabilizing more favorable geometries.

### Coupling of metal oxidation state with tertiary structure

Using the results of these calculations, we can speculate about a possible mechanism coupling the oxidation state with tertiary structure. In the case of cytochromes *c* (27, 28), for example, in which there is a reversible transition between oxidized and reduced forms (ferric and ferrous iron) during electron transport, we would predict that the redox potential will be sensitive to the geometry of the hydrogen bond—i.e., that a more favorable hydrogen bond geometry would result in a greater stabilization of the oxidized form. This prediction finds some support from our calculations of  $E_D$  using the x-ray coordinates of the few oxidized cytochromes for which structures are available. It is found that lower redox potentials are correlated with higher  $E_D$  values (R. P. Sheridan and L. C. Allen, unpublished results).

In the case of hemoglobin and myoglobin, the electron-

withdrawing character of the ligands that bind to the unliganded form—e.g.,  $O_2$  and CO—should result in a net shift of electrons away from the proximal histidine (29–32); we propose that this can also be modeled by an increase in positive charge (higher  $Z_X$ ) on the imidazole–formamide dimer. We conclude therefore, that the geometry of the hydrogen bond connecting the carbonyl oxygen of the leucine residue to the proximal histidine will be coupled at least to some extent with the affinity of the unliganded protein for these electron-withdrawing ligands.

One might go further and suggest that the geometry of this hydrogen bond may play a role in cooperative binding of ligands by hemoglobin by influencing  $c = K_R/K_T$ , the ratio of the ligand dissociation constants of the R (high-affinity) and T (low-affinity) states (33). Exactly how binding of ligands shifts the equilibrium between the T and R quaternary states and, conversely, how the quaternary state controls affinity remain unknown, although many reasonable suggestions have been made (34–43). To consider the relationship between hydrogen bond geometry and ligand binding, we must assume that the deoxy- hydrogen bond geometry is characteristic of the T state and the met- geometry is characteristic of the R state for both  $\alpha$  and  $\beta$  chains of hemoglobin (a strict two-state model). In addition, we assume that binding of electron-withdrawing ligands is equivalent to adding more positive charge to the hydrogen bond. The results for both  $\alpha$  and  $\beta$  chains of hemoglobin indicate that the met- geometry is more stabilized than the deoxy- geometry by an increase in positive charge (cationic minus neutral for met- is greater than for deoxy-, see Table 2). If the geometries are strictly associated with the quaternary states, we conclude that, according to our mechanism, binding of ligand would stabilize the R state more than the T state. Conversely, the R geometry more strongly favors ligand binding (the introduction of positive charge on the hydrogen bond) than would the T geometry. It is tempting to calculate a limiting estimate of the energy of cooperativity from the data in Table 2. The energy of cooperativity, for instance in oxygen binding, may be defined as the difference per subunit between the energies of the reactions  $T(\text{unliganded}) \rightarrow T(\text{oxy-})$  and  $R(\text{unliganded}) \rightarrow R(\text{oxy-})$ . In our case, we substitute the reactions deoxy geometry (neutral dimer)  $\rightarrow$  deoxy- geometry (cationic dimer) and met- geometry (neutral dimer)  $\rightarrow$  met- geometry (cationic dimer). This calculation gives approximately 3–4 kcal/mol per subunit as an upper limit of the energy of cooperativity due to this hydrogen bond, a value that happens to be quite close to the experimental value (33). We recognize, of course, that this is an extremely rough estimate due to uncertainties resulting from the choice of basis set, imprecision in the coordinates, and lack of information about the change in the positive charge on the hydrogen bond in going from the unliganded to the oxy- form. We also recognize that the ligands CO, NO, and  $O_2$ , which are known to produce similar energies of cooperativity (33), may not induce equal charge changes on this hydrogen bond. Nevertheless, we suggest that at least some of the energy of cooperativity in hemoglobin may be associated with the hydrogen bond and that the effect of such hydrogen bonds should be considered in constructing models for structure–activity relationships in hemoglobin.

The role of hydrogen bonds in the differential stabilization of oxidation states of other types of redox proteins should also be considered as more structures become available. Hydrogen bonds in iron–sulfur proteins, for instance, are reported to be associated with modulation of the redox potential (44–47). In this case the reduced state is stabilized by hydrogen bonds in which the electron donors are the sulfur atoms in the iron–sulfur cluster. Within this class of proteins the number of such hy-

drogen bonds is correlated with the redox potential (44, 47). In high potential iron-sulfur protein, the hydrogen bonds are in fact found to shorten upon reduction of the molecule (45, 46). Another redox protein in which hydrogen bonds may play such a role is flavodoxin, in which at least one hydrogen bond stabilizes the semiquinone form of the FMN coenzyme (48).

We are grateful to T. G. Spiro, J. J. Hopfield, J. A. Fee, M. Nappa, and H. T. Wright for helpful discussions and to M. Lopez for technical assistance. Financial support from the Charles and Johanna Busch Memorial Fund (to J.S.V.), U.S. Public Health Service Grant GM 24759 (to J.S.V.), National Science Foundation Grant PCN 76-23236 from the Biophysics Program of the Molecular Biology Section (to L.C.A.), the Rutgers University Research Council (to P.C.K.), a Biomedical Resources Support Grant (to P.C.K.), and the New Jersey State Agricultural Experiment Station (to P.C.K.) is also gratefully acknowledged. J.S.V. also acknowledges receipt of a U.S. Public Health Service Research Career Development Award.

1. Sundberg, R. J. & Martin, R. B. (1974) *Chem. Rev.* **74**, 471-517.
2. Quioco, F. A. & Lipscomb, W. N. (1971) *Adv. Protein Chem.* **25**, 1-78.
3. Richardson, J. S., Thomas, K. A., Rubin, B. H. & Richardson, D. C. (1975) *Proc. Natl. Acad. Sci. USA* **72**, 1349-1353.
4. Mathews, F. S., Argos, P. & Levine, M. (1971) *Cold Spring Harbor Symp. Quant. Biol.* **36**, 387-395.
5. Blumberg, W. E. & Peisach, J. (1971) *Adv. Chem. Ser.* **100**, 271-291.
6. Peisach, J., Blumberg, W. E. & Adler, A. (1973) *Ann. N. Y. Acad. Sci.* **206**, 310-326.
7. Peisach, J. (1975) *Ann. N. Y. Acad. Sci.* **244**, 187-202.
8. Peisach, J. & Mims, W. B. (1977) *Biochemistry* **16**, 2795-2799.
9. Walker, F. A., Lo, M.-W. & Ree, M. T. (1976) *J. Am. Chem. Soc.* **98**, 5552-5560.
10. Satterlee, J. D., LaMar, G. N. & Frye, J. S. (1976) *J. Am. Chem. Soc.* **98**, 7275-7282.
11. Metzler, D. E. (1977) *Biochemistry, The Chemical Reactions of Living Cells* (Academic, New York), pp. 566-567.
12. Nappa, M., Valentine, J. S. & Snyder, P. A. (1977) *J. Am. Chem. Soc.* **99**, 5799-5800.
13. Mohr, P., Scheler, W., Schumann, H. & Muller, K. (1967) *Eur. J. Biochem.* **3**, 158-163.
14. Swanson, R., Trus, B. L., Mandel, N., Mandel, G., Kallai, O. B. & Dickerson, R. E. (1977) *J. Biol. Chem.* **252**, 759-775.
15. Takano, T., Trus, B. L., Mandel, N., Mandel, G., Kallai, O. B., Swanson, R. & Dickerson, R. E. (1977) *J. Biol. Chem.* **252**, 776-785.
16. Mandel, N., Mandel, G., Trus, B. L., Rosenberg, J., Carlson, G. & Dickerson, R. E. (1977) *J. Biol. Chem.* **252**, 4619-4636.
17. Takano, T. (1977) *J. Mol. Biol.* **110**, 537-568.
18. Takano, T. (1977) *J. Mol. Biol.* **110**, 569-584.
19. Bolton, W. & Perutz, M. F. (1970) *Nature (London)* **228**, 551-552.
20. Ladner, R. C., Heidner, E. J. & Perutz, M. F. (1977) *J. Mol. Biol.* **114**, 385-414.
21. Makinen, M. N. (1975) in *Techniques and Topics in Bioinorganic Chemistry*, ed. McAuliffe, C. A. (Wiley, New York), pp. 3-106.
22. Kearns, R. C. & Allen, L. C. (1978) *J. Am. Chem. Soc.* **100**, 6587-6594.
23. Allen, L. C. (1975) *Proc. Natl. Acad. Sci. USA* **72**, 4701-4705.
24. Martinez-Carrera, S. (1966) *Acta Crystallogr.* **20**, 783-789.
25. The Chemical Society (1965) *Tables of Interatomic Distances and Configuration in Molecules and Ions*, Special Publication 18, (The Chemical Society, London).
26. Hehre, W. J., Lathan, W. A., Ditchfield, R., Newton, M. D. & Pople, J. A. (1973) *Quantum Chemistry Program Exchange* **9**, 236.
27. Dickerson, R. E. & Timkovich, R. (1975) in *The Enzymes*, ed. Boyer, P. D. (Academic, New York), 3rd Ed., Vol. 11, pp. 397-547.
28. Salemme, F. R. (1977) *Annu. Rev. Biochem.* **46**, 299-329.
29. Yamamoto, T., Palmer, G., Gill, D., Salmeeen, I. T. & Rimai, L. (1973) *J. Biol. Chem.* **248**, 5211-5213.
30. Caughey, W. S., Barlow, C. H., Maxwell, J. C., Volpe, J. A. & Wallace, W. J. (1975) *Ann. N. Y. Acad. Sci.* **244**, 1-8.
31. Collman, J. P., Brauman, J. I., Halbert, T. R. & Suslick, K. S. (1976) *Proc. Natl. Acad. Sci. USA* **73**, 3333-3337.
32. Demma, L. S. & Salhany, J. M. (1977) *J. Biol. Chem.* **252**, 1226-1230.
33. Weissbluth, M. (1974) *Hemoglobin Cooperativity and Electronic Properties*, Molecular Biology, Biochemistry and Biophysics (Springer, New York), Vol. 15.
34. Perutz, M. F. (1970) *Nature (London)* **228**, 726-734.
35. Perutz, M. F. (1972) *Nature (London)* **237**, 495-499.
36. Hopfield, J. J. (1973) *J. Mol. Biol.* **77**, 207-222.
37. Warshel, A. (1977) *Proc. Natl. Acad. Sci. USA* **74**, 1789-1793.
38. Gelin, B. R. & Karplus, M. (1977) *Proc. Natl. Acad. Sci. USA* **74**, 801-805.
39. Baldwin, J. M. (1975) *Prog. Biophys. Mol. Biol.* **29**, 225-320.
40. Edelstein, S. J. (1975) *Annu. Rev. Biochem.* **44**, 209-232.
41. Shulman, R. G., Hopfield, J. J. & Ogawa, S. (1975) *Q. Rev. Biophys.* **8**, 325-420.
42. Chothia, C., Wodak, S. & Janin, J. (1976) *Proc. Natl. Acad. Sci. USA* **73**, 3793-3797.
43. Collman, J. P., Brauman, J. I., Rose, E. & Suslick, K. S. (1978) *Proc. Natl. Acad. Sci. USA* **75**, 1052-1055.
44. Adman, E., Watenpaugh, K. D. & Jensen, L. H. (1975) *Proc. Natl. Acad. Sci. USA* **72**, 4854-4858.
45. Carter, C. W., Jr., Kraut, J., Freer, S. T. & Alden, R. A. (1974) *J. Biol. Chem.* **249**, 6339-6346.
46. Carter, C. W., Jr. (1977) *Iron-Sulfur Proteins III*, ed. Lovenberg, W. (Academic, New York), pp. 157-204.
47. Carter, C. W., Jr. (1977) *J. Biol. Chem.* **252**, 7802-7811.
48. Smith, W. W., Burnett, R. M., Darling, G. D. & Ludwig, M. L. (1977) *J. Mol. Biol.* **117**, 195-225.